Chapter 5
Design Considerations for Small Animal PET Scanners

Virginia Ch. Spanoudaki and Craig S. Levin

1 Introduction

Positron emission tomography (PET) is an established imaging technique currently used for the clinical management of disease in oncology, cardiology and neurology [1–3]. PET is nowadays integrated in the clinical routine and is acknowledged as a sensitive molecular imaging method. In addition to clinical applications, PET is also an active research tool in preclinical imaging with somewhat different applications. In order to highlight the specific goals of preclinical the following sub-sections will outline the differences between clinical and preclinical PET imaging in terms of applications and system performance requirements. Following that, this chapter will cover in more detail basic design considerations of preclinical PET scanners.

1.1 Applications

Preclinical PET plays a key role in the evaluation of new pharmaceuticals as well as in the assessment of the biological origin of various human diseases through imaging of appropriate animal models. Typically rodents (mice and rats) are used as

V.Ch. Spanoudaki
Department of Radiology, Molecular Imaging Program at Stanford (MIPS), Massachusetts Institute of Technology, Massachusetts, CA, USA
e-mail: vspan@mit.edu

C.S. Levin (✉)
Departments of Radiology, and by courtesy, Physics, Electrical Engineering, and Bioengineering; Molecular Imaging Instrumentation Laboratory (MIIL); Stanford Molecular Imaging Scholars (SMIS) Program; Stanford Center for Innovation in In-Vivo Imaging (SCI3); Molecular Imaging Program at Stanford (MIPS); Division of Nuclear Medicine, Stanford University School of Medicine, Stanford, CA, USA
e-mail: cslevin@stanford.edu

H. Zaidi (ed.), *Molecular Imaging of Small Animals: Instrumentation and Applications*,
DOI 10.1007/978-1-4939-0894-3_5,

such models due to their genetic similarity to humans [4, 5]; however primate imaging, typically monkeys, as well as imaging of other mammalians such as swine has also been reported [6, 7].

PET allows for non-invasive, in-vivo imaging of biological processes, thus each animal may be used for several different studies or the same study may be performed in the same animal over several days. In this way the experimental accuracy is improved and the number of sacrificed animals is reduced significantly resulting in a corresponding cost reduction of each study.

1.2 General Performance Requirements

Compared to clinical PET imaging the regions of interest under investigation in preclinical imaging are several orders of magnitude smaller. For that reason, the required spatial resolution of preclinical systems is accordingly higher. In addition, the specific activity (activity per unit mass) that may be administered to the animal is restricted due to limitations in the delivered dose. Proper detection of the limited amounts of activity requires high photon sensitivity of the imaging system, in order to be able to visualize and quantify as accurately as possible small amounts of radiotracer concentrations.

An ideal preclinical PET system should have the following characteristics:

- It should have *sub-millimeter spatial resolution* which should be uniform throughout the field of view. Thus the system should be able to detect lesions of all sizes with the same accuracy.
- Due to the limited amount of radioactivity administered to the animal, the ideal system should be able to detect a large fraction (optimally larger than 10 %) of the occurred annihilation events (*high photon sensitivity*), namely it should provide sufficient geometric coverage of the imaged animal and in addition it should absorb efficiently the energy of the emitted photons.
- If the system employs multiple small detector elements for improved spatial resolution, there should be an accurate correction for *non-uniformities* in the aforementioned photon efficiency among the various detector elements.
- It should be able to distinguish photons of different energies (*high energy resolution*, optimally smaller than 10 %) and precisely detect each annihilation photon's arrival time (*high time resolution*, optimally smaller than 1 ns).
- The system should respond linearly to a large range of photon emission rates with a *live-time* fraction of more than 95 %.
- The *system design* should allow for accurate readout of a large number of detector elements in a *cost effective* way.

These requirements pose a number of hardware design challenges which will be addressed in more detail in the following sections.

2 Specific Performance Requirements

2.1 Spatial Resolution and Partial Volume Effect

As mentioned above (Sect. 1.2) a spatial resolution below 1 mm is desired. For the majority of current system designs this is a rather difficult goal to achieve given the impractical small sizes of the detector elements required in combination with other blurring factors discussed in this section. The spatial resolution of an imaging system is a quantitative measure of the system's ability to localize a structure. It is defined as the minimum detectable size of a focal point of tracer accumulation or, otherwise stated, the minimum distance between two foci such that they can still be distinguished from each other (Fig. 5.1). Typical spatial resolutions (for a point source in the center with high statistics) of preclinical systems lie in the range between 1.5 and 2 mm, significantly smaller compared to the 4–8 mm resolution limits in clinical imaging [8–10] (where low statistics necessitate image smoothing), however recent advances in detector designs have led to sub-millimeter resolutions [11–13].

For systems based on discrete scintillation crystal elements read out by photodetectors, the intrinsic limit in spatial resolution is determined by the crystal element width. For systems based on alternative detector technologies, such as gas or semiconductor detectors, spatial resolution is determined by the pitch of the readout electrode wires, strips or pads.

The nature of positron annihilation poses some additional limitations to spatial resolution which are rather difficult to be addressed by technical approaches. The first is the positron range, namely the finite distance that the positron traverses inside a subject prior to its annihilation. This distance depends on the positron maximum energy E_{max} as well as on the tissue in which the positron migrates. The larger E_{max} is, the larger the positron range variance within a specific tissue thus causing degradation of the spatial resolution. Studies have shown that for the widely used ^{18}F positron emitter ($E_{max} = 635$ keV), the positron range in water has a distribution with 0.1 mm full width at half maximum (FWHM), which is well below the current spatial resolution limits of both clinical and preclinical PET [14].

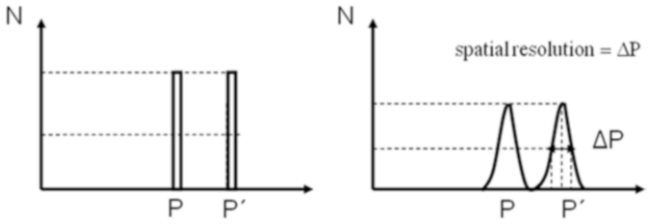

Fig. 5.1 Illustration of the concept of spatial resolution: the ideal intensity profiles of two neighboring point sources (*left*) appear in reality smoother (*right*) due to the imaging system's spatial resolution. The latter is defined as the FWHM of the resulting intensity profile. If two adjacent profiles are separated by a distance greater than ΔP, the point sources will be resolved

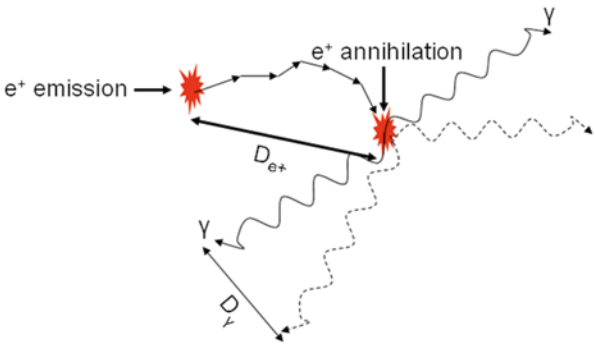

Fig. 5.2 Effect of positron range and photon acolinearity on spatial resolution of PET. Their variations contribute to spatial resolution blurring. The respective spatial blurring components D_{e+} and D_γ contribute in quadrature to the achievable spatial resolution

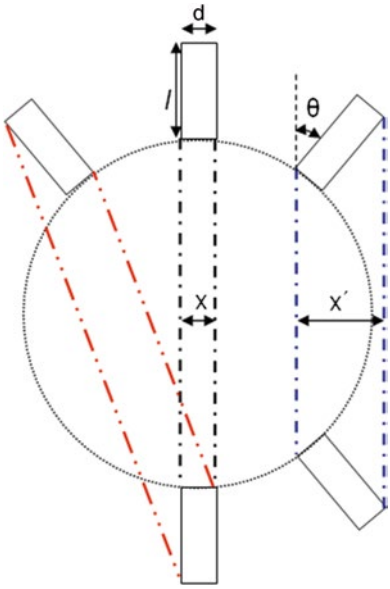

Fig. 5.3 Illustration of the parallax effect for lines of response (LoRs) with different obliqueness. For a non-oblique detector pair the depth of interaction of the 511 keV photons along the detector length *l* does not affect the width *x* of the ToR (*black dashed lines*). For oblique detector pairs the ToR width *x′* broadens (*red* or *blue dashed lines*) depending on the crystal element length (*l*) and element size (*d*) as well as on the detector obliqueness θ and the angle of photon incidence

During annihilation of a positron with an electron there is the possibility that the two produced annihilation photons are emitted at an angle with respect to each other which slightly deviates from 180° due to residual positron or electron momentum. This photon acolinearity produces a spatial deviation that increases linearly with the tomograph's diameter and thus is more prominent in clinical PET [14, 15]. As in positron range, it is the variance in this deviation that further degrades spatial resolution. Both the effects of positron range and photon acolinearity are illustrated in Fig. 5.2.

The length of the crystal element also affects the spatial resolution of a PET system, especially for small fields of view (FoV), such as in preclinical PET. The so called parallax error, namely the non-uniformity of spatial resolution throughout the FoV is illustrated in Fig. 5.3. The finite crystal element length and the penetration of the 511 keV photons in the crystal volume, translate to an uncertainty of where

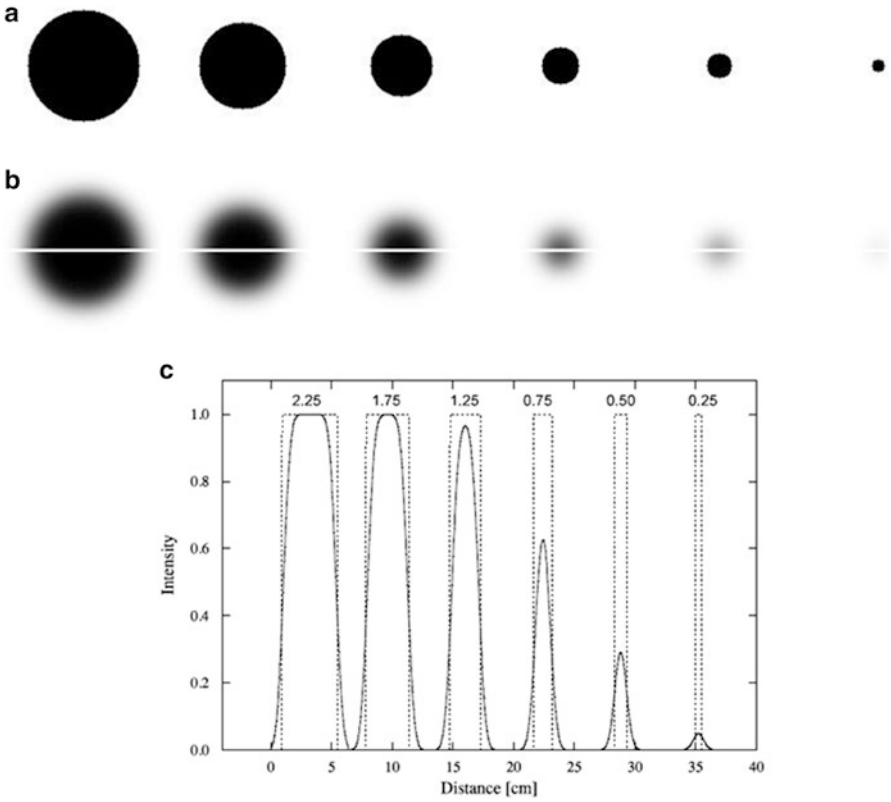

Fig. 5.4 Illustration of the partial volume effect. (**a**) Simulated spheres of different sizes and the same activity concentration. (**b**) Reconstructed images of the spheres imaged by a 10 mm resolution system. (**c**) Position profiles of the images shown in (**b**) indicating that the activity concentration appears to be smaller for smaller objects. Reproduced from [16] with permission

within the width of the response tube (ToR) defined by a detector element pair the positron annihilation took place.

A side effect of the limited spatial resolution in PET is the so called partial volume effect (PVE), illustrated in Fig. 5.4. PVE is the underestimation of the radioactivity concentration in a region of interest (RoI) in the reconstructed image if this RoI is smaller than the spatial resolution of the system. PVE effects can also lead to overestimation of the radioactivity concentration depending on the background surrounding the RoI [16].

2.2 Photon Sensitivity

Photon sensitivity of a PET system is the ratio of the detected coincident photon pair event rate (measured in counts per second or cps) to the emitted radioactivity from the object to be imaged (measured in Ci or Bq). However it is common to quote

absolute photon sensitivity as the percentage (%) of emitted coincident photons that are detected. The ideal photon sensitivity limit (>10 %) mentioned in Sect. 1.2 still deviates significantly from the typically achieved values given the limited solid angle coverage as well as the inherently limited detector intrinsic photon detection efficiency.

In general, radiation detection is a process dominated by Poisson statistics and therefore, in the case of PET imaging, it will inevitably result in fluctuations in photon sensitivity. Because in Poisson statistics any fluctuation or variance is directly associated with the mean value, the photon sensitivity fluctuations in a PET system are associated with the mean detected number of coincident events. A general rule is that the relative fluctuations on the mean detected number of radiation events over this mean value is inversely proportional to the square root of this mean. Thus it is desirable that photon detection systems have high photon sensitivity (high mean detected number of photon events) in order to minimize statistical variations. Typical photon sensitivities of preclinical systems lie in the range between 1 and 7 % and are significantly larger than the typical values of clinical systems due to the smaller system diameter and thus the larger solid angle coverage of the imaged object. This fact allows the use of small detector elements in preclinical imaging while maintaining an adequate number of detected counts per element.

One of the most important factors which affect the photon sensitivity of a system is the crystal material. The effective atomic number Z and the density ρ of the material define its photon stopping power and thus the intrinsic detector efficiency. High Z and high ρ values are desired for enhanced possibility of absorption of the emitted annihilation photons in the detector material. In addition, the obliqueness of a detector with respect to the incident radiation as well as the inevitable dead space between detectors affects the intrinsic efficiency. Additional to the intrinsic efficiency, the geometric efficiency of the PET system plays a large role to the overall photon sensitivity. Systems with detectors placed as close as possible to the object to be imaged (i.e. small ring diameter for cylindrical systems) and with a radial/axial extent are typically designed in order to enhance the overall photon sensitivity.

The actual sensitivity of a PET system will be further degraded by the fact that not all registered coincident events are actually the ones we want; depending on the energy and time resolution of the system, which will be explained in more detail in Sects. 2.3 and 2.4, true coincidences will be contaminated by background scattered and accidental coincident photon events. The former coincidence type originates from scatter of one or both of the annihilation photons within the imaged object thus resulting in detection of the two photons from a different detector pair. In order to avoid such localization errors, scattered coincidences are rejected by setting a proper threshold in the recorded photon energies. The latter coincidence type is a false coincidence between two photons that originate from two independent positron annihilations which happen to occur within the same time window. Accidental coincidences may be rejected by setting a proper time coincidence window. The different types of coincident events (true, random and scattered coincidences) are outlined in Fig. 5.5.

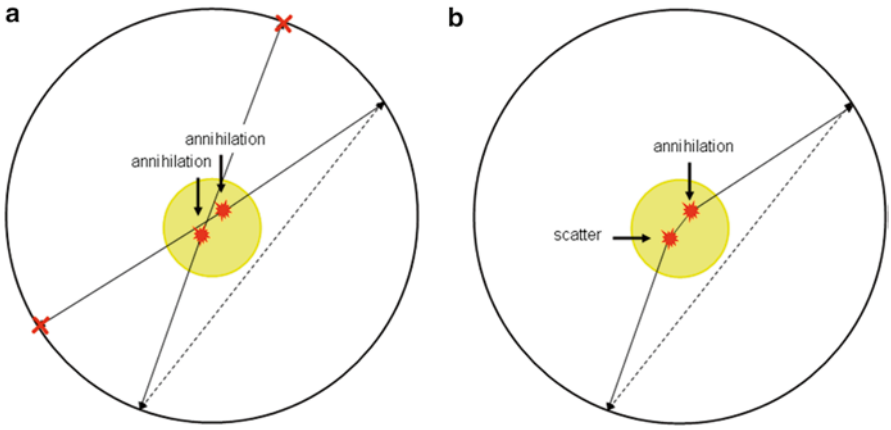

Fig. 5.5 (**a**) Random coincidences: two photon events registered within the same time window may result in the assignment of a LoR (*dashed line*) even though the two events originate from independent annihilations. (**b**) Scatter coincidences: the scatter of one or both annihilation photons may result in localization errors by assigning a LoR to a different detector pair than the expected one (*dashed line*)

Two-dimensional (2D) acquisition mode was performed by the early clinical PET systems in order to reduce the number of registered random or scattered coincidences. In this mode, only coincidences between detectors belonging to the same detector element ring (direct plane coincidences) or to the immediate neighboring rings (cross-plane coincidences) are registered. Thus the number of scattered or random coincidences is decreased significantly, however so is the good or "true" photon sensitivity. Modern PET systems adopt the three-dimensional (3D) acquisition mode in which coincidences between all detector pairs (belonging to any detector element ring) are registered. This acquisition mode greatly enhances the system's photon sensitivity; however accurate corrections for scattered and random coincidences are necessary.

A PET system comprises of many individual detectors and thus variations in photon detection efficiency among the various detectors may be observed. Even though minor differences in the intrinsic detection efficiency are possible from crystal to crystal, the vast majority of variations may be observed either due to their position in the PET system or due to intrinsic detector gain variations.

2.3 Energy Resolution

The accuracy at which a PET system responds to a specific amount of photon energy absorbed by its detectors defines its energy resolution. One of the requirements, outlined in Sect. 1.2, for an ideal preclinical PET system was an energy resolution of less than 10 %. Especially for standard system designs based on scintillation

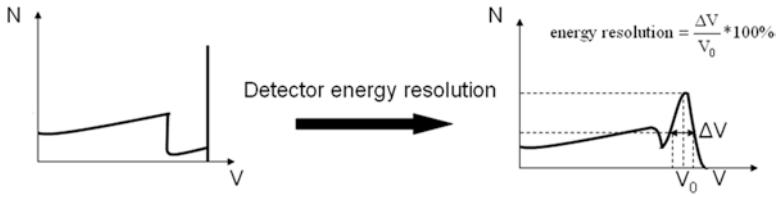

Fig. 5.6 Illustration of the concept of energy resolution: an ideal histogram of the deposited energies in the detector (including both Compton scatter and photoelectric absorption) is shown on the *left drawing*. The detector response on the absorbed 511 keV photon energy (photopeak) is a "delta function". The limited energy resolution of the detector results in a histogram similar to the one shown on the *right drawing*. The photopeak follows approximately a Gaussian distribution

crystal readout by photodetectors the relatively low conversion efficiency of the incident photon energy to electric charge results in energy resolution degradation, so that typical energy resolutions for these designs lie between 15 and 25 %. In PET the energy of interest is 511 keV, namely the energy of each of the two anti-parallel annihilation photons per event, thus resolution is typically defined with respect to this energy.

For a detector with ideal (infinitively precise) energy resolution, a histogram of the PET system's response to the absorbed 511 keV energy (in form of collected detector charge or detector pulse height) would be a "spike" at a single energy (such "spikes" are mathematically described by the so-called delta function). However for a detector with non-ideal energy resolution, the 511 keV line will appear to have a Gaussian distribution with a FWHM of, typically, several tens of keV about the 511 keV value (Fig. 5.6).

In a PET system employing many detectors, differences in the energy resolution values characterizing each individual detector may be observed. These differences are most commonly attributed to gain and noise variations between the photodetectors and if not properly identified and corrected for, they may hinder the system's ability to represent in a quantitative way the true radiotracer concentration.

Energy information requires a high level of accuracy in order to properly distinguish scattered from unscattered events. The former will deposit only part of their energy in the detector while the latter will fully deposit their energy. The worse (higher value) the energy resolution the more difficult it is to distinguish scatter from photopeak events. Scattered events lead to localization errors as outlined in Fig. 5.5b and subsequently to a uniform background in the reconstructed image thus affecting image contrast, signal to noise ratio (SNR) and quantitative accuracy.

The annihilation photons may scatter both in the object to be imaged as well as in the crystal material itself. Although scatter in small animals is less than in humans due to the smaller object volume within the FoV, the effect is still significant [17]. Crystal scatter is apparent in both clinical and especially preclinical PET since the crystal elements are smaller. As previously mentioned, given adequate energy resolution, the effects of object scatter, which effectively lead to mispositioning of annihilation events, is reduced. However, scatter in the crystal may still be exploited to

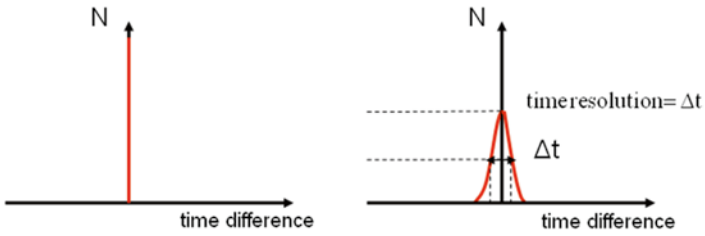

Fig. 5.7 Illustration of the concept of time resolution: Ideally the time difference between two photon detection events that occurred simultaneously would be zero, thus a histogram of the time differences over many simultaneous events would be a delta function centered around zero (*left*). Due to the system's limited time resolution the histogram appears to be smooth following a Gaussian distribution (*right*)

identify annihilation events provided that the position of the first interaction can be determined. Detector designs based on individual readout of finite crystal elements have the ability of identification of crystal scatter [18, 19].

2.4 Time Resolution

PET imaging is based on coincident photon detection and thus photon arrival time information needs to be extracted as accurately as possible. In counting systems whose detection principle is based on the measured time difference between detector signals, such as PET systems, the precision to which this time difference is determined is of utmost importance. This precision is directly related to the PET detector's time (or temporal) resolution which is defined as the uncertainty to which the arrival time of an event is estimated by the detector system (Fig. 5.7). Recent advances in improving the response speed of scintillators and photodetectors have made the desired time resolution limits mentioned in Sect. 1.2 feasible.

Typically, time information about the occurrence of an event is extracted from the produced detector voltage signal $V(t)$. The time resolution is then described by the following formula:

$$\sigma_t = \sqrt{\left(\frac{\sigma_V}{\frac{dV}{dt}}\right)^2 + \sigma_{TTS}^2} \tag{5.1}$$

where σ_V is the signal root-mean-square (RMS) noise, $\frac{dV}{dt}$ is the signal slope at the point of time pick-off and σ_{TTS} is the transit time variance of the optical photons within the scintillation crystal and the electric charge within the photodetector. As it can be seen from the above formula, the time resolution of a single PET detector depends on a number of parameters:

– The light output, the decay time and the geometry of the scintillator. A scintillator with high optical photon rate (eventually translated as $\frac{dV}{dt}$ in the detector output) will reduce the effect of statistical variations (on the amount of light contributing to σ_V in the detector output) in the determination of the arrival time and will allow timing pick-off at early stages of scintillation photon production. The crystal geometry, and more specifically the crystal aspect ratio (width-to-length ratio), is also an important factor. A crystal with high aspect ratio will minimize the variation in distance between the point of optical photon production and the point of optical photon detection. Thus with short crystal elements photon losses at the crystal interfaces (affecting V) and flight time variations (as reflected by σ_{TTS}) are minimized.
– The noise (represented by σ_V), gain (represented by V) and transit time spread (represented by σ_{TTS}) of the photodetector or any other means used to detect the annihilation photons, such as gas or semiconductor crystals.

As already outlined in the previous section for the case of energy resolution, in a complete PET system, which employs several (hundreds to thousands) detector and electronic channels, the overall system time resolution will be affected by the individual detector time resolutions and indeed might be broadened due to inherent temporal shifts between detectors. Proper correction of these temporal variations through a procedure known as time calibration will minimize the system time resolution for coincidence detection from all possible detector pairs in the system.

In PET imaging it is essential that time resolution is kept as low as possible in order to minimize contamination of true coincident photon events from accidental (random) coincidences. The latter typically add a uniform background in the PET reconstructed image thus reducing image contrast, SNR and quantitative accuracy. From theory, the number of random coincidences increases proportionally to the time coincidence window and to the product of event flux seen by each detector in a coincident detector pair. Thus, minimization of random events requires that the time coincidence window selected for coincidence detection be as low as possible and the activity is as low as possible.

In addition to controlling the accidental coincidence rate, the time resolution poses a lower limit in the minimum temporal difference between two subsequent coincident photon events in order for the detector to identify them as distinct. However this minimum time difference between events is further degraded by the detector recovery time as well as by the dead time of the subsequent electronics, as will be explained in more detail in Sect. 3.4.

Detectors that demonstrate sub-nanosecond time resolution are currently used in clinical imaging in order to exploit the actual time of flight (ToF) information of the two annihilation photons and improve the SNR of the reconstructed image. The benefits of ToF are more obvious for large sized patients however the current time resolution limitations of PET detectors limit the applicability of ToF methodology to clinical PET only.

Table 5.1 summarizes the aforementioned performance requirements and compares their significance for clinical and preclinical PET.

Table 5.1 Summary of the performance parameters in PET imaging and significance in clinical and preclinical PET

Feature	Clinical PET	Preclinical PET
Spatial resolution	4–8 mm	1–2 mm
Effect of time resolution (randoms/count rate)	Significant	Not as significant (depends on application)
Effect of energy resolution (scatter)	Significant	Not as significant
Photon sensitivity	$O(10^{-2})$	$O(10^{-2})$
Effect of DoI	For points close to detectors	Significant
Effect of ToF	In image SNR	Currently none

3 Detector Designs

3.1 Materials

The fundamental components of PET detectors have been reviewed in detail in previous chapters of this book. In the following sections, we will summarize the various detector configurations employed in PET scanners, we will outline their advantages and disadvantages and emphasize the significance of their special features in preclinical PET imaging.

3.1.1 Scintillation Crystal–Photodetector

The large majority of PET systems consist of detectors whose basic components are a scintillation crystal coupled to a photodetector. This detector configuration provides an indirect means of detection of 511 keV photons through the two-step process of conversion to scintillation light via a scintillation crystal and a subsequent conversion to electric charge via a photodetector. Through this multi-step process inevitable signal losses and additional statistical variations and dispersions are introduced. Nevertheless, to date a scintillator/photodetector configuration is the standard choice in the design of PET systems [15].

As described, scintillators with high effective atomic number (Z), density (ρ), light output and short decay time are preferred for optimum PET performance in terms of time/energy resolution and photon sensitivity. A major breakthrough in PET detector technology has been enabled with the invention of fast inorganic scintillators such as lutetium oxyorthosilicate (LSO) which demonstrates a good compromise between high light output and fast timing. However, its natural radioactivity may pose a number of design issues which nevertheless are addressed without implying significant design limitations [20, 21].

Photomultiplier tubes (PMTs) have mostly been used as the preferred photodetectors due to their excellent performance features (see Chap. 3). However, their relatively large sizes result in large dead spaces and thus poor packing fraction. This has motivated the development of specialized detector designs where the readout of

the scintillation light by the PMT is interfaced by means of a light guide [22]. In this way, good crystal packing fraction is guaranteed independent of the gaps between photodetectors. This is of particular importance in the case of preclinical scanners where the available space is limited by the small system diameters. A new generation of preclinical PET systems is based upon Avalanche Photodiodes (APDs) due to their availability in small sizes and compact arrays allowing thus for direct interfacing between the miniscule scintillator elements and the photodetector. An additional advantage of APDs over PMTs is that the former are able to operate reliably under the presence of magnetic fields which makes them appropriate for simultaneous PET/MRI, as will be emphasized in Chap. 15.

3.1.2 Gas Filled Detectors

In order to overcome the inevitable signal losses of the aforementioned indirect scintillation detection methods, researchers have looked into alternative detection techniques. The architecture of multiwire proportional counters (MWPCs) used in high energy physics experiments have been implemented in the quad-HIDAC small animal PET scanner [11].

Lead honey-comb structures are used to convert the 511 keV photons into electrons. The charge subsequently migrates within a gas medium under the influence of an electric field and is detected by a network of anode electrodes. A major advantage of such systems is the high spatial resolution defined by the electrode pitch which however comes at the expense of energy information, poor time resolution and poor photon sensitivity.

3.1.3 Semiconductor Detectors

Another detector configuration employing direct conversion of 511 keV photons to charge are semiconductor detectors. Semiconductor detectors such as germanium (Ge) or cadmium telluride (CdT) can be highly efficient in 511 keV detection resulting in excellent energy resolution [23]. Currently there is increasing interest in the latter material for high resolution PET because it operates in room temperature and, similar to MWPCs, sub-millimeter intrinsic spatial resolutions may be achieved due to the fine pitch of the anode and/or cathode electrodes. The poor time resolution of these detectors is however still a limitation [10].

Figure 5.8 shows pictures of the three different PET detector types.

3.2 Readout Designs

Since the most common detector components are scintillation crystals with photodetector readout, our discussion in the following sub-sections will focus on readout configurations of designs based on those components.

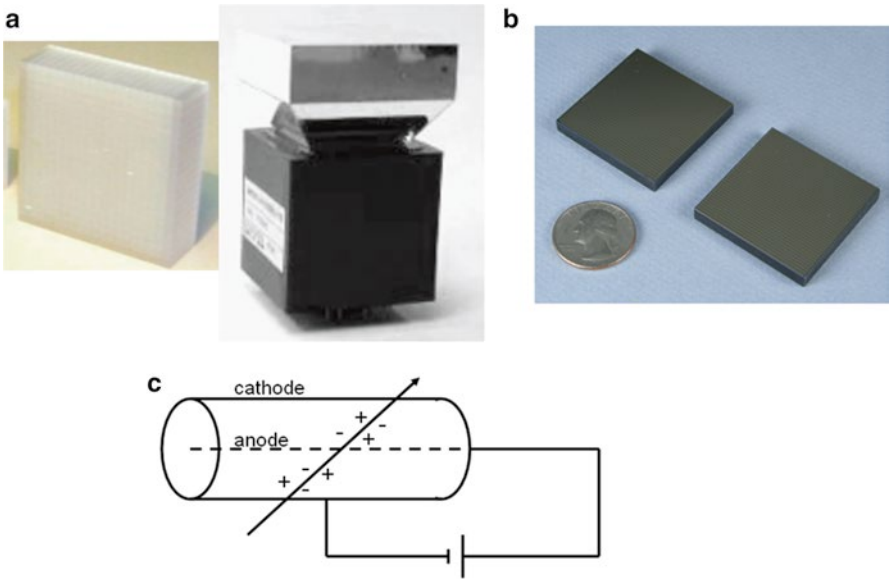

Fig. 5.8 Three different detector types currently used in preclinical PET systems: (**a**) *left*: 20×20 LSO crystal array (crystal element size 1.5×1.5×10 mm^3). *Right*: LSO crystal array, tapered light guide and PSPMT (courtesy of Robert Nutt, Siemens Preclinical Solutions). (**b**) Anode view of two CZT detectors (courtesy of Yi Gu, Stanford University). (**c**) Basic detection principle of gas-filled detectors

3.2.1 Block Detector Readout

The block detector design refers to the indirect readout of many crystal array elements by a fewer number of photodetectors based on scintillation light sharing. Three different block detector designs can be identified:

– Readout of a crystal slab by a number of photodetectors [15, 24]. The scintillation light produced by the interaction of a 511 keV photon with the crystal is shared among the various photodetectors and information about the position of interaction is extracted by the relative amplitudes of the different photodetector signals and is estimated using appropriate positioning algorithms. This design is based on the Anger gamma camera architecture and its advantage lies in the simplicity of its implementation [15].
– Readout of a crystal array by a coarse photodetector array [15]. In the same way as in the previous design the scintillation light produced in crystal array elements is shared among the various photodetectors and the position information is extracted by positioning algorithms. However, in this case the crystal elements are optically isolated using reflectors and the scintillation light is thus more focused and confined within the volume of one or two crystal elements. Thus light sharing among the photodetectors should be facilitated by means of an

additional optical medium, typically a light guide in between the crystal array and the photodetector.
– Alternative to photodetector arrays, position sensitive photodetectors, such as position sensitive photomultiplier tubes (PSPMTs) [25, 26] or position sensitive avalanche photodiodes (PSAPDs) may be used [27]. These photodetectors consist of a single photosensitive area (as opposed to the discrete elements in an array) whose produced charge is collected by multiple anodes or a resistive charge multiplexing network connecting the anodes. This network will yield a number of signals (typically four) which are subsequently used in conjunction with positioning algorithms for interaction localization. This design, which is apparent in most clinical and preclinical PET systems, offers the advantage of significant reduction of the readout channels while using a large number of small scintillation crystal elements for improved spatial resolution.

Some disadvantages of the block detector readout scheme are the dependence of position localization accuracy, and consequently of spatial resolution, on the algorithm used and on the effectiveness of the light sharing with respect to electronic SNR. Additionally, in cases of high counting rates, block detectors are sensitive to pulse pile up effects as will be explained in Sect. 3.4.2. Finally, this design cannot differentiate between object scatter and scatter in the crystal. The latter is an effect that is especially important in preclinical PET systems since the crystal elements are small and scatter in small animal tissues is less likely than in patients.

3.2.2 Individual Crystal Readout

A limited number of PET scanners have adopted the individual crystal readout scheme where the crystal elements are coupled one-to-one to the photodetectors [28]. This readout scheme overcomes the positioning limitations of block detectors because the detector intrinsic spatial resolution is determined by the scintillation crystal element size. Unlike block detectors, in this detector design intercrystal scatter mentioned in Sect. 2.3 can be identified. In addition, detectors with individual crystal readout are capable of higher count rates (less pulse pile up) compared to block detectors given the fact that each photodetector reads a single scintillation crystal element. However the aforementioned advantages come at the expense of increased number of detector and electronic channels which further implies increased costs as well as construction and signal processing complexity.

Figure 5.9 depicts the various aforementioned detector designs. The PET detectors are typically arranged in ring geometry to allow acquisition from different angular views (Fig. 5.10a). However initial alternative PET system architectures suggest arrangement of the PET detectors in partial ring geometry (Fig. 5.10b) [29]. Tomographic acquisition is performed by rotating the detectors around the animal. Partial ring geometries can be more cost effective although the overall duration of the PET scan can be significantly increased and rotational artifacts may be introduced. It is also possible to arrange detectors into other shapes, such as a box [30].

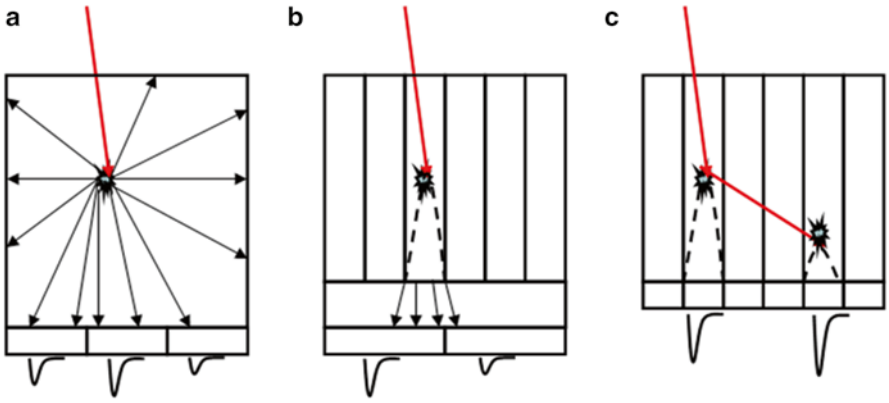

Fig. 5.9 (**a**) Block detector readout of a crystal slab, (**b**) block detector readout of a crystal array, (**c**) individual crystal readout

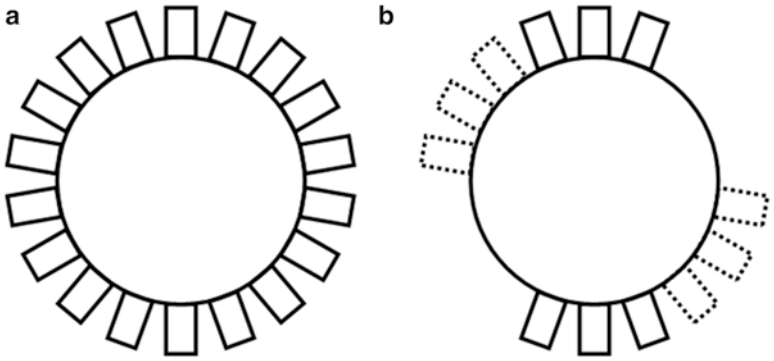

Fig. 5.10 PET system designs. (**a**) Full ring geometry, (**b**) partial ring geometry. The detectors marked with a *dashed line* indicate different rotation for tomographic acquisition

3.3 Special Design Features

The need for increased quantitative accuracy in preclinical PET has lead to the development of specific detector designs aimed to address a number of current limitations. In the following, the discussion will focus on design features which compensate for non uniform spatial resolution and motion artifacts.

3.3.1 Depth of Interaction

In PET scanners with small FoV, especially in preclinical tomographs, significant spatial resolution non-uniformity across the FoV may be observed depending on the radial extent (or length) of the scintillation crystal element used and the radial

position within the system. This effect is called the parallax error and is illustrated in Fig. 5.3. The exponential attenuation of the 511 keV photons in the scintillation crystal implies a statistical likelihood of the interaction along the crystal length with enhanced probability close to the photon's entrance point and exponentially decreasing probability with increasing distance from that point. Thus, in a crystal of finite length the exact interaction point is not known, but rather its likelihood results in an additional position blurring especially for oblique photon incidence that occurs for emission points away from the center [10].

As emphasized in Sect. 2.2, PET photon sensitivity is enhanced by the use of long (thick) crystals of high atomic number and density. Consequently, there is a trade-off between photon sensitivity and spatial resolution uniformity which is successfully addressed by a number of specialized detector designs described in the following:

– Dual ended crystal readout: A common DoI detector design employs crystal elements read out by two photodetectors on both sides [31]. In this way the depth of interaction of the annihilation photon inside the crystal is determined by the difference in the amount of light detected by the two photodetectors. An advantage of this method is the availability of continuous DoI information; however the light sharing between the two photodetectors may result in poor detector performance in terms of energy and/or timing resolution. Positioning nonlinearity near the two photodetectors is also apparent in this design. In addition, detailed detector calibration (particularly with respect to gain variability between the two photodetectors) is a prerequisite for extraction of reliable DoI information.
– Individual crystal readout: This detector design has been adopted as a straightforward method of acquiring quantized DoI information [32]. The design consists of two or more crystal layers each read out by individual photodetectors. The DoI resolution is determined by the dimension of the crystal layer along the radial direction and at the same time the detector performance is maintained due to the individual readout. However, the basic drawback of this design is the increasing number of electronic readout channels and thus the potential development costs. Alternatively, the crystal layers are read out collectively by position sensitive photodetectors [33, 34]. Such designs are more cost effective given the reduced number of readout channels compared to the number of crystal elements in the detectors, and they provide much better DoI resolution.
– Phoswich design: The phoswich detector comprises two different types of scintillation crystal materials read out by the same photodetector [35, 36]. Identification of the crystal of interaction (and thus DoI) is realized by pulse shape discrimination given the different decay time constants of the two scintillation crystal types. A major drawback of this detector design is the interdetector performance variability due to the different types of scintillation material used. This variability may especially hinder timing performance given the fact that one of the crystals should have a slower decay time compared to the other.
– Monolithic crystal design: More recently there have been detector designs based on a single monolithic crystal layer read out by either individual photodetectors

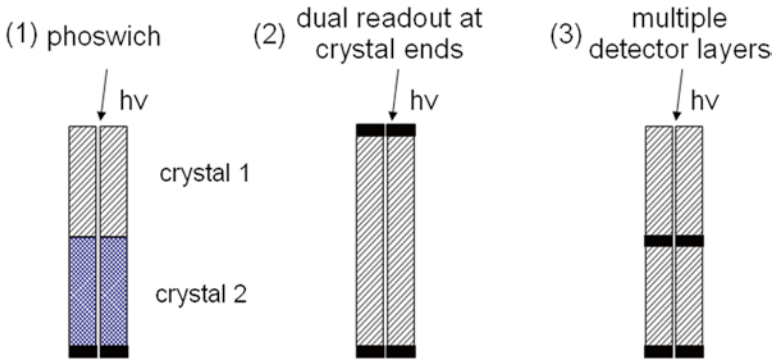

Fig. 5.11 Detector designs with DoI capabilities. (*1*) Phoswich, (*2*) dual ended crystal readout, (*3*) individual crystal readout of layered detectors

or position sensitive photodetectors employing a resistive network able to identify the scintillation light spread profile on the photodetector entrance surface [24, 37–39]. The light spread profile depends on the depth of interaction and several algorithms have been developed that associate the acquired profiles with DoI [38, 39]. Despite the detector simplicity implied by the use of a single monolithic crystal layer, the complexity of this design lies mostly in the photodetector readout scheme and the associated algorithms and calibrations. In addition this design is subject to the general spatial resolution limitations, especially near corners and edges, as are all designs employing continuous crystals.

The most common DoI detector designs are summarized in Fig. 5.11.

3.3.2 Motion Correction

Quantitative studies performed in PET require accurate calculation of the radiotracer distribution within a region of interest. The RoI is typically drawn based on the reconstructed image, thus its accuracy will directly depend on the quality and accuracy of the PET image.

Quantitative accuracy dictates that a number of corrections be performed post acquisition and during reconstruction. Apart from the rejection of scattered and random coincident events, as well as attenuation correction, localization errors may originate from inevitable movement of the imaged object such as respiration and cardiac motion. Especially in the case of preclinical imaging, the heart beat and respiration rates are significantly higher compared to humans (60–100 heartbeats/min and 15–20 respirations/min for humans vs. approximately 500 heartbeats/min and 160 respirations/min for mice). This fact, in combination with the higher spatial resolution of small animal systems makes the imaging system performance more sensitive to motion artifacts.

Several methods for motion correction have been developed from various groups [40–42]. Typically, for cardiac motion ECG sensors are used and respiratory motion is monitored via motion sensors placed near the abdominal area of the animal. List

mode data acquisition, namely acquisition of the energy and time of individual photon events in a list, is suitable for incorporating the motion sensors' signal into the data stream. The list mode data is then rearranged in groups belonging to the same stage of each cardiac/breathing cycle during the course of measurement in order to produce images free of motion artifacts.

3.4 Data Acquisition Electronics

The signals produced by the PET detectors are further processed by subsequent electronics in order to extract two types of information: Energy, as represented by the integrated pulse height, and time, as represented by the signal time stamp. The latter is essential in PET for determining coincident photon pairs from single photon events whereas the former is used to identify and remove scatter events that may degrade image quality and accuracy. Even though the first PET scanners based their acquisition chain in coincidence detection hardware modules, modern systems record single photon events and their corresponding energy and time information (list-mode data format) and coincidence detection is performed either in software post-acquisition or in field programmable gate array (FPGA) based hardware architectures during or post-acquisition. The basic issues that need to be addressed when designing data acquisition systems for PET are the number of electronic channels and the processing speed as reflected by the system's dead time.

Typically the current or charge produced by the photodetector is converted to a voltage signal with the use of preamplifiers. These preamplifiers provide a pulse in their output whose height is typically proportional to the photodetector charge which in turn is proportional to the scintillation crystal light and thus to the absorbed incident photon energy. Especially in the case of low gain detectors the preamplifier needs to be placed as close as possible to the detector in order to avoid signal attenuation. A charge sensitive preamplifier integrates the photodetector charge through a capacitor (C) and a resistive load (R) for a time window defined by the time constant $\tau = RC$. Typically, the R and C values are chosen in such a way so that the integration occurs for a time window at least three times larger compared to the scintillation decay time. The resulting pulse will have a rising edge following the photodetector response and a trailing edge dominated by the time constant τ.

Subsequent electronics are used to further shape the signal, mainly increasing SNR and restoring a faster return to the baseline. The shaped signal is used for the extraction of energy and time information by means of a peak detector circuit for the former and a time pick-off circuit for the latter. All the aforementioned steps of the electronic chain require a minimum processing time for each detector signal affecting thus the overall system dead time.

More recent data acquisition systems are based on sampling of the shaped signal and extracting energy and time information from the digitized samples based on various algorithms applied either in software or in FPGAs. This acquisition option leads to increased flexibility in the choice of processing algorithms, however it may result in increased cost and analysis complexity following acquisition.

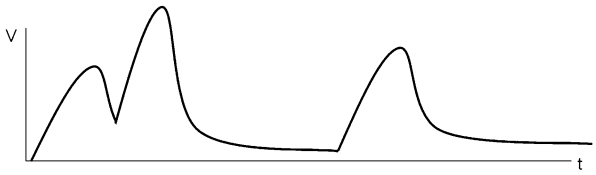

Fig. 5.12 Illustration of the signal pile up effect. The finite scintillator decay time dictates a signal charge integration time of typically at least two to three times the decay time, resulting in pulses with a relatively long trailing edge. In cases of high counting rates the possibility of detector pulses adding to the trailing edge of the preceding pulse increases, resulting in distorted pulse shapes

3.4.1 Signal Multiplexing

The need to reduce the number of electronic channels in the described detector designs (Sects. 3.2.1 and 3.2.2) has lead to the development of several channel reduction techniques at the front end readout electronics [43, 44]. For front-end channel reduction, signals from multiple photodetector channels are multiplexed either resistively or capacitively. Special care is given to the design of the multiplexing architectures so that the multiplexed signals carry accurate position information and at the same time lead to minimal degradation of energy and time resolution. Successful signal multiplexing schemes have lead to a four-fold or higher reduction on the number of electronic channels.

3.4.2 Signal Pile Up and Dead Time Effects

In imaging situations involving high amounts of tracer radioactivity, such as cardiac imaging, the response of the data acquisition system to high counting rates may be subject to signal pile up and dead time effects. Specifically these effects are more prominent in preclinical PET systems due to the smaller system diameter and thus higher photon sensitivity.

Signal pile up occurs mainly at the early stages of the signal processing chain. If the intensity of the incident photon flux is such that the detection of a photon event, and the associated generation of a detector signal, occurs before a signal from a previous detection has returned to its baseline, the former will be superimposed on the trailing edge of the previous detector signal, as illustrated in Fig. 5.12. The pulse shape is thus distorted resulting in inaccurate information about both the height and time of the pulse. Pulse pile up is significantly suppressed by reducing the duration of the pulse trailing edge via appropriate shaping. In Sect. 3.2.1 it was pointed out that block detector designs are more subject to pile up effects compared to designs with individual crystal readout. This is due to the fact that in the former design each photodetector reads out the scintillation photon fluxes from multiple crystals. In moderate count rates pile up is not apparent given the fact that it is rather unlikely that two crystals seen by the same photodetector in a PET system will produce signals close together in time.

Dead time is usually defined as the minimum temporal difference between two events in order for the imaging system to identify them as two separately detected events. Dead time is essentially a property of the imaging system as a whole, originating from both the detector front end and the data acquisition electronics.

Detector dead time is related to the recovery of the scintillator and the photodetector after the detection of a photon event. Data acquisition dead time is related to the time it takes for the peak detector, time pick-off circuits, digitizers and data transfer architectures to reset in order to be able to process the next event.

Counting systems can be distinguished in terms of their dead time behavior, in two different categories [23]:

- Paralyzable systems: if two or more events are incident within a time window which is smaller than the minimum processing time required for that system, the system will not process any events during this time window. Thus the system's dead time is effectively increased depending on the rate of incident events.
- Non-paralyzable systems: if two or more events are incident within a time window which is smaller than the minimum processing time required for that system, the system will process those events as a single event.

Depending on the complexity of the PET data acquisition system, its dead time may not belong to either of the above categories. Several groups have been working in developing appropriate dead time models for specific PET systems in order to correct for counting losses [45].

4 State-of-the-Art Preclinical Systems

A number of preclinical PET tomographs initially developed by research groups have been commercialized and are currently used by several research centers around the world.

- **MicroPET/Focus/Inveon (CTI/Siemens):** The MicroPET technology is based on pixellated LSO crystals readout by PSPMTs by means of optical fibers. Different versions of this technology varying in crystal and FoV sizes have been realized [46–48].
- **Mosaic (Philips):** This system is based on GSO pixellated crystals coupled to hexagonal arrays of individual PMTs via a continuous light guide [49].
- **Argus (Suinsa):** The Argus system is the first commercially available PET system employing DoI capability [50]. Its detector architecture consists of a dual phoswich detector (LYSO/LGSO) read out by PSPMTs.
- **ClearPET (Raytest):** This preclinical system also employs DoI capabilities by means of a phoswich detector (LYSO/LuYAP) read out by PSPMTs [51]. The scanner has adjustable FoV allowing thus for both rodent and primate imaging.
- **LabPET (Gamma Medica-Ideas):** The LabPET system is the first commercially available APD based PET scanner. The system employs a phoswich detector (LYSO/LGSO) where the two different crystals are arranged next to each other in order to read out two detectors with the same APD [52].

Table 5.2 Performance summary of commercially available preclinical PET systems

System	Detector material	Radial FoV (mm)	Axial FoV (mm)	Transaxial/axial spatial resolution @ center (mm)	Photon sensitivity (%)
MicroPET	LSO	112	18	1.8, 2.0	0.56 @ 250 keV
Focus	LSO	258	76	1.3, 1.3	3.4 @ 250 keV
Inveon	LSO	161	127	<1.8	9.3 @ 250 keV
Mosaic	GSO	197	128	2.7, 3.4	0.65 @ 410 keV
Argus	LYSO/GSO	118	48	1.4	2.1 @ 400 keV
ClearPET	LYSO/LuYAP	135	110	1.3	4.5 @ 250 keV
LabPET	LYSO/LGSO	100	37.5/75	1.4, 1.3	1/2 @ 250 keV
Quad-HiDAC	Lead/Argon gas	170	280	1.1	1.0 @ 0 keV
FLEX™	BGO	100	118	1.8–2.0	8 @ 250 keV

– **Quad HiDAC (Oxford Positron Systems):** The quad-HiDAC system, also mentioned in Sect. 3.1.2, makes use of gas detectors equipped with lead converters and read out by electrode meshes. The system achieves sub-millimeter spatial resolution despite the poor time resolution, no energy resolution and poor photon sensitivity [11].
– **FLEX™ (Gamma Medica-Ideas):** The XPET system of the tri-modality FLEX™ tomograph (PET/SPECT/CT) consists of a detector ring based on quadrant sharing of BGO crystal arrays by arrays of PMTs. The detector block has the shape of a pentagon with tapered ends resulting in high detector packing fraction [53].

Table 5.2 summarizes quantitatively the basic performance features of these systems. Several other research systems employ special features:

– **RatCAP:** The Rat Conscious Animal PET (RatCAP) is a prototype PET scanner aimed to perform brain studies in conscious rats thus avoiding anesthesia which may inhibit several brain processes under study. Its architecture is based on individual readout of LSO crystal arrays by APD arrays with the detectors fixed in the animal's skull [54].
– **VP-PET:** The Virtual Pinhole PET (VP-PET) is a technology aiming to improve the spatial resolution of already existing systems by implementing a high resolution detector insert within the FoV [55]. Coincidences are registered between all possible detector pairs from both the existing system and the insert resulting in magnification similar to pinhole SPECT [56–59].

5 Summary

In this chapter, an overview of the design considerations for small animal PET scanners was given. Preclinical imaging is widely used in PET research for the evaluation of new pharmaceuticals and for the study of the biology of various human diseases.

However, the performance requirements for preclinical imaging differ from those for clinical imaging due to the significantly different volumes to be imaged. Differences in energy, time and spatial resolution between preclinical and clinical PET were explained and current trends in the PET detector designs were presented. A summary of state-of-the-art small animal PET scanners was also given.

Acknowledgments This work was supported by the National Institutes of Health (NIH) with grants R01CA119056 from NCI, R33EB003283 from NIBIB, R01CA120474 from NCI and P50CA114747 from NCI. The authors would also like to acknowledge the support of GE Healthcare and the AXA Research Fund.

References

1. Chen W (2007) Clinical applications of PET in brain tumors. J Nucl Med 48:1468-81.
2. Schwaiger M, Ziegler S, Nekolla SG (2005) PET/CT: challenge for nuclear cardiology. J Nucl Med 46:1664-78.
3. Strauss LG, Conti PS (1991) The applications of PET in clinical oncology. J Nucl Med 32:623-48; discussion 649-50.
4. Pellegrino D, Cicchetti F, Wang X, Zhu A, Yu M, Saint-Pierre M, et al. (2007) Modulation of dopaminergic and glutamatergic brain function: PET studies on Parkinsonian rats. J Nucl Med 48:1147-53.
5. Stegger L, Hoffmeier AN, Schafers KP, Hermann S, Schober O, Schafers MA, et al. (2006) Accurate noninvasive measurement of infarct size in mice with high-resolution PET. J Nucl Med 47:1837-44.
6. Fowler JS, Kroll C, Ferrieri R, Alexoff D, Logan J, Dewey SL, et al. (2007) PET studies of d-methamphetamine pharmacokinetics in primates: comparison with l-methamphetamine and (--)-cocaine. J Nucl Med 48:1724-32.
7. Munk OL, Bass L, Roelsgaard K, Bender D, Hansen SB, Keiding S (2001) Liver kinetics of glucose analogs measured in pigs by PET: importance of dual-input blood sampling. J Nucl Med 42:795-801.
8. Brix G, Zaers J, Adam LE, Bellemann ME, Ostertag H, Trojan H, et al. (1997) Performance evaluation of a whole-body PET scanner using the NEMA protocol. National Electrical Manufacturers Association. J Nucl Med 38:1614-23.
9. Levin CS (2005) Primer on molecular imaging technology. Eur J Nucl Med Mol Imaging 32 Suppl 2:S325-45.
10. Levin CS (2008) New imaging technologies to enhance the molecular sensitivity of positron emission tomography. Proceedings of the IEEE 96:439-467.
11. Schafers KP, Reader AJ, Kriens M, Knoess C, Schober O, Schafers M (2005) Performance evaluation of the 32-module quadHIDAC small-animal PET scanner. J Nucl Med 46:996-1004.
12. Stickel JR, Qi J, Cherry SR (2007) Fabrication and characterization of a 0.5-mm lutetium oxyorthosilicate detector array for high-resolution PET applications. J Nucl Med 48:115-21.
13. Visvikis D, Lefevre T, Lamare F, Kontaxakis G, Santos A, Darambara D (2006) Monte Carlo based performance assessment of different animal PET architectures using pixellated CZT detectors. Nucl Instr Meth A 569:225-229.
14. Levin CS, Hoffman EJ (1999) Calculation of positron range and its effect on the fundamental limit of positron emission tomography system spatial resolution. Phys Med Biol 44:781-99.
15. Cherry SR, Phelps ME, Sorenson JA (2003) *Physics in nuclear medicine*, 3rd ed. Philadelphia, PA: Saunders.

16. Phelps ME (2004) *PET molecular imaging and its biological applications*. New York: Springer.
17. Yang YF, Cherry SR (2006) Observations regarding scatter fraction and NEC measurements for small animal PET. IEEE Trans Nucl Sci 53:127-132.
18. Pratx G, Levin CS (2009) Bayesian reconstruction of photon interaction sequences for high-resolution PET detectors. Phys Med Biol 54:5073-94.
19. Rafecas M, Boning G, Pichler BJ, Lorenz E, Schwaiger M, Ziegler SI (2003) Inter-crystal scatter in a dual layer, high resolution LSO-APD positron emission tomograph. Phys Med Biol 48:821-48.
20. Huber JS, Moses WW, Jones WF, Watson CC (2002) Effect of 176Lu background on singles transmission for LSO-based PET cameras. Phys Med Biol 47:3535-41.
21. Watson CC, Casey ME, Eriksson L, Mulnix T, Adams D, Bendriem B (2004) NEMA NU 2 performance tests for scanners with intrinsic radioactivity. J Nucl Med 45:822-6.
22. Surti S, Karp JS, Freifelder R, Liu F (2000) Optimizing the performance of a PET detector using discrete GSO crystals on a continuous lightguide. IEEE Trans Nucl Sci 47: 1030-1036.
23. Knoll GF (2000) *Radiation detection and measurement*, 3rd ed. New York ; Toronto: Wiley.
24. Joung J, Miyaoka RS, Lewellen TK (2002) cMiCE: a high resolution animal PET using continuous LSO with a statistics based positioning scheme. Nucl Instr Meth A 489:584-598.
25. Monzo JM, Lerche CW, Martinez JD, Esteve R, Toledo J, Gadea R, et al. (2009) Analysis of time resolution in a dual head LSO plus PSPMT PET system using low pass filter interpolation and digital constant fraction discriminator techniques. Nucl Instr Meth A 604: 347-350.
26. Seidel J, Vaquero JJ, Barbosa F, Lee IJ, Cuevas C, Green MV (2000) Scintillator identification and performance characteristics of LSO and GSO PSPMT detector modules combined through common X and Y resistive dividers. IEEE Trans Nucl Sci 47:1640-1645.
27. Levin CS (2002) Design of a high-resolution and high-sensitivity scintillation crystal array for PET with nearly complete light collection. IEEE Trans Nucl Sci 49:2236-2243.
28. Pichler BJ, Bernecker F, Boning G, Rafecas M, Pimpl W, Schwaiger M, et al. (2001) A 4×8 APD array, consisting of two monolithic silicon wafers, coupled to a 32-channel LSO matrix for high-resolution PET. IEEE Trans Nucl Sci 48:1391-1396.
29. Ziegler SI, Pichler BJ, Boening G, Rafecas M, Pimpl W, Lorenz E, et al. (2001) A prototype high-resolution animal positron tomograph with avalanche photodiode arrays and LSO crystals. Eur J Nucl Med 28:136-43.
30. Habte F, Foudray AM, Olcott PD, Levin CS (2007) Effects of system geometry and other physical factors on photon sensitivity of high-resolution positron emission tomography. Phys Med Biol 52:3753-72.
31. Yang Y, Dokhale PA, Silverman RW, Shah KS, McClish MA, Farrell R, et al. (2006) Depth of interaction resolution measurements for a high resolution PET detector using position sensitive avalanche photodiodes. Phys Med Biol 51:2131-42.
32. Rafecas M, Boning G, Pichler BJ, Lorenz E, Schwaiger M, Ziegler SI (2001) A Monte Carlo study of high-resolution PET with granulated dual-layer detectors. IEEE Trans Nucl Sci 48: 1490-1495.
33. Zhang J, Foudray AMK, Cott PD, Farrell R, Shah K, Levin CS (2007) Performance characterization of a novel thin position-sensitive avalanche photodiode for 1 mm resolution positron emission tomography. IEEE Trans Nucl Sci 54:415-421.
34. Zhang J, Olcott PD, Chinn G, Foudray AM, Levine CS (2007) Study of the performance of a novel 1 mm resolution dual-panel PET camera design dedicated to breast cancer imaging using Monte Carlo simulation. Med Phys 34:689-702.
35. Mosset JB, Devroede O, Krieguer M, Rey M, Vieira JM, Jung JH, et al. (2006) Development of an optimized LSO/LuYAP phoswich detector head for the Lausanne ClearPET demonstrator. IEEE Trans Nucl Sci 53:25-29.

36. Seidel J, Vaquero JJ, Green MV (2003) Resolution uniformity and sensitivity of the NIH ATLAS small animal PET scanner: Comparison to simulated LSO scanners without depth-of-interaction capability. IEEE Trans Nucl Sci 50:1347-1350.
37. Lerche CW, Benlloch JM, Sanchez F, Pavon N, Escat B, Gimenez EN, et al. (2005) Depth of gamma-ray interaction within continuous crystals from the width of its scintillation light-distribution. IEEE Trans Nucl Sci 52:560-572.
38. Maas MC, Schaart DR, van der Laan DJ, Bruyndonckx P, Lemaitre C, Beekman FJ, et al. (2009) Monolithic scintillator PET detectors with intrinsic depth-of-interaction correction. Phys Med Biol 54:1893-908.
39. Schaart DR, van Dam HT, Seifert S, Vinke R, Dendooven P, Lohner H, et al. (2009) A novel, SiPM-array-based, monolithic scintillator detector for PET. Phys Med Biol 54:3501-12.
40. Lucignani G (2009) Respiratory and cardiac motion correction with 4D PET imaging: shooting at moving targets. Eur J Nucl Med Mol Imaging 36:315-9.
41. Dawood M, Kosters T, Fieseler M, Buther F, Jiang X, Wubbeling F, et al. (2008) Motion correction in respiratory gated cardiac PET/CT using multi-scale optical flow. Med Image Comput Comput Assist Interv 11:155-62.
42. Lamare F, Cresson T, Savean J, Cheze Le Rest C, Reader AJ, Visvikis D (2007) Respiratory motion correction for PET oncology applications using affine transformation of list mode data. Phys Med Biol 52:121-40.
43. Pichler BJ, Swann BK, Rochelle J, Nutt RE, Cherry SR, Siegel SB (2004) Lutetium oxyorthosilicate block detector readout by avalanche photodiode arrays for high resolution animal PET. Phys Med Biol 49:4305-19.
44. Siegel S, Silverman RW, Shao YP, Cherry SR (1996) Simple charge division readouts for imaging scintillator arrays using a multi-channel PMT. IEEE Trans Nucl Sci 43:1634-1641.
45. Daube-Witherspoon ME, Carson RE (1991) Unified deadtime correction model for PET. IEEE Trans Med Imaging 10:267-75.
46. Bao Q, Newport D, Chen M, Stout DB, Chatziioannou AF (2009) Performance evaluation of the Inveon dedicated PET preclinical tomograph based on the NEMA NU-4 standards. J Nucl Med 50:401-8.
47. Cherry SR, Shao Y, Silverman RW, Meadors K, Siegel S, Chatziioannou A, et al. (1997) MicroPET: A high resolution PET scanner for imaging small animals. IEEE Trans Nucl Sci 44:1161-1166.
48. Tai YC, Ruangma A, Rowland D, Siegel S, Newport DF, Chow PL, et al. (2005) Performance evaluation of the microPET Focus: a third-generation microPET scanner dedicated to animal imaging. J Nucl Med 46:455-63.
49. Huisman MC, Reder S, Weber AW, Ziegler SI, Schwaiger M (2007) Performance evaluation of the Philips MOSAIC small animal PET scanner. Eur J Nucl Med Mol Imaging 34:532-40.
50. Wang Y, Seidel J, Tsui BM, Vaquero JJ, Pomper MG (2006) Performance evaluation of the GE healthcare eXplore VISTA dual-ring small-animal PET scanner. J Nucl Med 47:1891-900.
51. Roldan PS, Chereul E, Dietzel O, Magnier L, Pautrot C, Rbah L, et al. (2007) Raytest ClearPET (TM), a new generation small animal PET scanner. Nucl Instr Meth Phys Res A 571: 498-501.
52. Bergeron M, Cadorette J, Beaudoin JF, Lepage MD, Robert G, Selivanov V, et al. (2009) Performance evaluation of the LabPET APD-based digital PET scanner. IEEE Trans Nucl Sci 56:10-16.
53. Parnham KB, Chowdhury S, Li J, Wagenaar DJ, Patt BE (2006) Second-generation, tri-modality, pre-clinical imaging system. NSS/MIC Conf Rec: 1802-1805
54. Vaska P, Woody CL, Schlyer DJ, Shokouhi S, Stoll SP, Pratte JF, et al. (2004) RatCAP: Miniaturized head-mounted PET for conscious rodent brain imaging. IEEE Trans Nucl Sci 51:2718-2722.
55. Tai YC, Wu H, Pal D, O'Sullivan JA (2008) Virtual-pinhole PET. J Nucl Med 49:471-9.
56. Beekman FJ, van der Have F, Vastenhouw B, van der Linden AJ, van Rijk PP, Burbach JP, et al. (2005) U-SPECT-I: a novel system for submillimeter-resolution tomography with radiolabeled molecules in mice. J Nucl Med 46:1194-200.

57. DiFilippo FP (2008) Design and performance of a multi-pinhole collimation device for small animal imaging with clinical SPECT and SPECT-CT scanners. Phys Med Biol 53: 4185-4201.
58. Palmer J, Wollmer P (1990) Pinhole emission computed tomography: method and experimental evaluation. Phys Med Biol 35:339-50.
59. Shokouhi S, Metzler SD, Wilson DW, Peterson TE (2009) Multi-pinhole collimator design for small-object imaging with SiliSPECT: a high-resolution SPECT. Phys Med Biol 54:207-225.